

Generation of Aeroservoelastic Reduced Order Models Using Time Scaling

Daniel C. Hammerand^{*} James M. Gariffo[†] Kevin M. Roughen[‡] and Myles L. Baker[§]

M4 Engineering, 4020 Long Beach Blvd., Long Beach, CA, 90807, USA

Oddvar O. Bendiksen[¶]

*Department of Mechanical and Aerospace Engineering
UCLA, 420 Westwood Plaza, Los Angeles, CA, 90095 USA*

Design of modern control laws motivates the creation of state-space models from aeroservoelastic models. Balanced truncation is often used to create reduced-order models. In the present work, a reduced order model that employs time scaling in computing the balancing transformation is developed. The transformation matrix necessary to transform the original (unscaled) aeroservoelastic model is found from that corresponding to the time scaled model. Results from an aeroservoelastic wing and a supersonic transport model are shown and it is demonstrated that with an appropriate choice of time scaling, the methodology results in greatly improved conditioning for the Lyapunov equations used to find the Gramians employed in the balancing transformation.

I. Introduction

THE design of modern flight vehicles requires sophisticated mathematical models. Aeroservoelastic models combine aerodynamics, controls, and structural models into a single model that can be used for control law design. The importance of performing active control for flutter suppression, gust load alleviation, and ride quality enhancement was identified during the NASA High Speed Research (HSR) program.^{1,2} The design of control laws for this class of vehicles continues.³ Ultimately, state-space models will be required.

The size of such aeroservoelastic models can be quite large (on the order of thousands of states⁴) and, thus, unsuitable for control law design. One approach for reduction is to compute a balanced realization followed by truncation. The balanced realization applied in the present research involves computing the controllability and observability Gramians of the aeroservoelastic model. Once these Gramians are computed, an eigenvalue problem is solved for the transformation matrix that results in the balanced states being ordered in terms of their controllability and observability.⁵⁻⁷ It is in this stage that the truncation may be performed safely by eliminating the modes with the least controllability and observability.

Previous research has developed aeroservoelastic reduced order models (ROMs) that are appropriate for control law design.⁴ In the present work, time scaling is applied to the previously developed ROMs in order to better condition the Lyapunov equations which are used to compute the Gramians. However, in order to avoid problems associated with new units for the physical dimension of time, the original unscaled system is the one that is balanced and truncated.

II. Unscaled Linear Time Invariant (LTI) System of Equations

The aeroservoelastic state-space model is generated using the methodology presented in Ref. 4. Essentially, the finite element method is used to compute the structural modal mass, stiffnesses, and damping

^{*}Senior Engineer, Research, dhammerand@m4-engineering.com, AIAA senior member

[†]Engineer, Research, jgariffo@m4-engineering.com, AIAA student member

[‡]Vice President of Engineering, kevin.roughen@m4-engineering.com, AIAA member

[§]President & Chief Engineer, mbaker@m4-engineering.com, and AIAA Associate Fellow

[¶]Professor, oddvar@seas.ucla.edu, AIAA Associate Fellow.

matrices, whereas the Doublet-Lattice method is used to generate a potential flow solution to the unsteady system aerodynamics.^{8,9} The aerodynamic data is converted to state-space form using a Rational Function Approximation (RFA).¹⁰ The structural and aerodynamic state-space models are combined along with a state-space model for the control surfaces. As shown in Ref. 4, the state-space set of equations considering acceleration to be the output is given as follows:

$$\begin{Bmatrix} \dot{\xi} \\ \ddot{\xi} \\ \dot{z} \end{Bmatrix} = \begin{bmatrix} 0 & I & 0 \\ -\widehat{M}^{-1}\widehat{K} & -\widehat{M}^{-1}\widehat{C} & q_\infty \widehat{M}^{-1}C_A \\ 0 & B_A^1 & A_A \end{bmatrix} \begin{Bmatrix} \xi \\ \dot{\xi} \\ z \end{Bmatrix} + \begin{bmatrix} 0 \\ \widehat{M}^{-1}r^T k \\ 0 \end{bmatrix} \{\delta_{cmd}\} \quad (1)$$

and

$$\{\ddot{y}\} = \begin{bmatrix} -\Phi\widehat{M}^{-1}\widehat{K} & -\Phi\widehat{M}^{-1}\widehat{C} & q_\infty\Phi\widehat{M}^{-1}C_A \end{bmatrix} \begin{Bmatrix} \xi \\ \dot{\xi} \\ z \end{Bmatrix} + \begin{bmatrix} \Phi\widehat{M}^{-1}r^T k \end{bmatrix} \{\delta_{cmd}\} \quad (2)$$

where the dot refers to time derivatives taken with respect to the physical time scale, t . In Eqs. (1) and (2), $\{\xi\}$ is the vector of generalized deflections, $\{\dot{\xi}\}$ is the vector of generalized velocities, $\{z\}$ is the vector of aerodynamic lag states, $\{\delta_{cmd}\}$ is the vector of control surface motions, and $\{\ddot{y}\}$ is the vector of nodal accelerations that are output. Also, in Eqs. (1) and (2), $[r]$ is a matrix converting the generalized deflection vector $\{\xi\}$ into unit deflection of the control surfaces and $[k]$ is a matrix of control surface gains. Furthermore, $[\widehat{M}]$, $[\widehat{C}]$, $[\widehat{K}]$ are given by

$$[\widehat{M}] = [\widetilde{M}] - [D_A^2] \quad (3)$$

$$[\widehat{C}] = [\widetilde{C}] - [D_A^1] + [r]^T [k] [a] [r] \quad (4)$$

$$[\widehat{K}] = [\widetilde{K}] - [D_A^0] + [r]^T [k] [r] \quad (5)$$

where $[a]$ is a matrix of control surface delay constants, and $[\widetilde{M}]$, $[\widetilde{C}]$, and $[\widetilde{K}]$ are the modal mass, damping, and stiffness matrices given by

$$[\widetilde{M}] = [\Phi]^T [M] [\Phi] \quad (6)$$

$$[\widetilde{C}] = [\Phi]^T [C] [\Phi] \quad (7)$$

$$[\widetilde{K}] = [\Phi]^T [K] [\Phi] \quad (8)$$

with $[M]$, $[C]$, $[K]$ representing the assembled mass, damping, and stiffness matrices, respectively, $[\Phi]$ representing the matrix of modal eigenvectors defined by the generalized eigenvalue problem

$$[K]\{\phi\} = \omega^2[M]\{\phi\} \quad (9)$$

and $[A_A]$, $[B_A^1]$, $[C_A]$, $[D_A^0]$, $[D_A^1]$, and $[D_A^2]$ representing the state-space system for the unsteady aerodynamics.

The system of state space equations is written in compacted notation as follows:

$$\begin{Bmatrix} \dot{\xi} \\ \ddot{\xi} \\ \dot{z} \end{Bmatrix} = [A] \begin{Bmatrix} \xi \\ \dot{\xi} \\ z \end{Bmatrix} + [B] \{\delta_{cmd}\} \quad (10)$$

and

$$\{\ddot{y}\} = [C] \begin{Bmatrix} \xi \\ \dot{\xi} \\ z \end{Bmatrix} + [D] \{\delta_{cmd}\} \quad (11)$$

where $[A]$, $[B]$, $[C]$, and $[D]$ are given respectively by

$$[A] = \begin{bmatrix} 0 & I & 0 \\ -\widehat{M}^{-1}\widehat{K} & -\widehat{M}^{-1}\widehat{C} & q_\infty \widehat{M}^{-1}C_A \\ 0 & B_A^1 & A_A \end{bmatrix} \quad (12)$$

$$[B] = \begin{bmatrix} 0 \\ \widehat{M}^{-1}r^T k \\ 0 \end{bmatrix} \quad (13)$$

$$[C] = \begin{bmatrix} -\Phi\widehat{M}^{-1}\widehat{K} & -\Phi\widehat{M}^{-1}\widehat{C} & q_\infty\Phi\widehat{M}^{-1}C_A \end{bmatrix} \quad (14)$$

and

$$[D] = \begin{bmatrix} \Phi\widehat{M}^{-1}r^T k \end{bmatrix} \quad (15)$$

If instead of acceleration, displacement is requested as the output, the set of linear output equations are given by

$$\{y\} = [\Phi \ 0 \ 0] \begin{Bmatrix} \xi \\ \dot{\xi} \\ z \end{Bmatrix} = [C] \begin{Bmatrix} \xi \\ \dot{\xi} \\ z \end{Bmatrix} \quad (16)$$

Likewise, if velocity is desired as the output, the linear output equations are given by

$$\{\dot{y}\} = [0 \ \Phi \ 0] \begin{Bmatrix} \xi \\ \dot{\xi} \\ z \end{Bmatrix} = [C] \begin{Bmatrix} \xi \\ \dot{\xi} \\ z \end{Bmatrix} \quad (17)$$

This system of equations potentially has conditioning problems regardless of the output. For instance, if

$$[\widehat{M}^{-1}\widehat{K}]_{ij} \gg 1 \quad \text{for some } i, j \quad (18)$$

then the resulting system of equations likely will be ill-conditioned and the Gramian calculations will likely be in error. In order to overcome this problem, the time dimension of the state-space model is scaled appropriately for use in computing the controllability and observability Gramians.

III. Time Scaled System of Equations

To achieve better conditioning for computing the Gramians, the time scale is converted to a different time scale, τ , where

$$\tau = \alpha t \quad (19)$$

For instance, if t is in seconds, choosing $\alpha = 1000$ gives τ in milliseconds. The first order time derivatives in Eqs. (1) and (2) will be transformed as follows:

$$\frac{d\xi}{dt} = \frac{d\xi}{d(\frac{1}{\alpha}\tau)} = \alpha \frac{d\xi}{d\tau} \quad (20)$$

and

$$\frac{dz}{dt} = \frac{dz}{d(\frac{1}{\alpha}\tau)} = \alpha \frac{dz}{d\tau} \quad (21)$$

Likewise, the second order time derivative becomes

$$\frac{d^2\xi}{dt^2} = \frac{d}{d(\frac{1}{\alpha}\tau)} \left(\frac{d\xi}{d\tau} \right) = \alpha^2 \frac{d^2\xi}{d\tau^2} \quad (22)$$

Letting $(\cdot)' = d(\cdot)/d\tau$, we have

$$\begin{Bmatrix} \xi \\ \dot{\xi} \\ z \end{Bmatrix} = \begin{bmatrix} I & 0 & 0 \\ 0 & \alpha I & 0 \\ 0 & 0 & I \end{bmatrix} \begin{Bmatrix} \xi \\ \xi' \\ z \end{Bmatrix} = [R] \begin{Bmatrix} \xi \\ \xi' \\ z \end{Bmatrix} \quad (23)$$

and

$$\begin{Bmatrix} \dot{\xi} \\ \ddot{\xi} \\ \dot{z} \end{Bmatrix} = \begin{bmatrix} \alpha I & 0 & 0 \\ 0 & \alpha^2 I & 0 \\ 0 & 0 & \alpha I \end{bmatrix} \begin{Bmatrix} \xi' \\ \xi'' \\ z' \end{Bmatrix} = \alpha [R] \begin{Bmatrix} \xi' \\ \xi'' \\ z' \end{Bmatrix} \quad (24)$$

Incorporating the change in the time scale, the state-space system of equations become

$$\begin{Bmatrix} \xi' \\ \xi'' \\ z' \end{Bmatrix} = \frac{1}{\alpha} [R]^{-1} [A] [R] \begin{Bmatrix} \xi \\ \xi' \\ z \end{Bmatrix} + \frac{1}{\alpha} [R]^{-1} [B] \{\delta_{cmd}\} \quad (25)$$

$$= [\tilde{A}] \begin{Bmatrix} \xi \\ \xi' \\ z \end{Bmatrix} + [\tilde{B}] \{\delta_{cmd}\} \quad (26)$$

and

$$\{s\} = \frac{1}{\beta} [C] [R] \begin{Bmatrix} \xi \\ \xi' \\ z \end{Bmatrix} + [D] \{\delta_{cmd}\} \quad (27)$$

$$= [\tilde{C}] \begin{Bmatrix} \xi \\ \xi' \\ z \end{Bmatrix} + [\tilde{D}] \{\delta_{cmd}\} \quad (28)$$

where

$$\{s\} = \begin{cases} \{y\} & \text{displacement output} \\ \{y'\} & \text{velocity output} \\ \{y''\} & \text{acceleration output} \end{cases} \quad (29)$$

and

$$\beta = \begin{cases} 1 & \text{displacement output} \\ \alpha & \text{velocity output} \\ \alpha^2 & \text{acceleration output} \end{cases} \quad (30)$$

Considering the acceleration to be the requested output, the system of state-space equations can be written explicitly as

$$\begin{Bmatrix} \xi' \\ \xi'' \\ z' \end{Bmatrix} = \begin{bmatrix} 0 & I & 0 \\ -\frac{1}{\alpha^2} \widehat{M}^{-1} \widehat{K} & -\frac{1}{\alpha} \widehat{M}^{-1} \widehat{C} & \frac{q_\infty}{\alpha^2} \widehat{M}^{-1} C_A \\ 0 & B_A^1 & \frac{1}{\alpha} A_A \end{bmatrix} \begin{Bmatrix} \xi \\ \xi' \\ z \end{Bmatrix} + \begin{bmatrix} 0 \\ \frac{1}{\alpha^2} \widehat{M}^{-1} r^T k \\ 0 \end{bmatrix} \{\delta_{cmd}\} \quad (31)$$

and

$$\{y''\} = \begin{bmatrix} -\frac{1}{\alpha^2} \Phi \widehat{M}^{-1} \widehat{K} & -\frac{1}{\alpha} \Phi \widehat{M}^{-1} \widehat{C} & \frac{q_\infty}{\alpha^2} \Phi \widehat{M}^{-1} C_A \end{bmatrix} \begin{Bmatrix} \xi \\ \xi' \\ z \end{Bmatrix} + \begin{bmatrix} \frac{1}{\alpha^2} \Phi \widehat{M}^{-1} r^T k \end{bmatrix} \{\delta_{cmd}\} \quad (32)$$

If, however, displacement or velocity is desired, the output equation respectively becomes

$$\{y\} = \begin{bmatrix} \Phi & 0 & 0 \end{bmatrix} \begin{Bmatrix} \xi \\ \xi' \\ z \end{Bmatrix} \quad (33)$$

or

$$\{y'\} = \begin{bmatrix} 0 & \Phi & 0 \end{bmatrix} \begin{Bmatrix} \xi \\ \xi' \\ z \end{Bmatrix} \quad (34)$$

IV. System Stability

As should be intuitively obvious, the fact that the stability classification of the system is unaffected by changing the time scale will be shown mathematically in the present section. Recall that the stability of the unscaled system is obtained by examining the eigenvalues of $[A]$. If all of the eigenvalues of $[A]$ have negative real parts, the system is stable. The relevant eigenvalue problems for the unscaled and time-scaled systems respectively are

$$[A]\{v\} = \lambda\{v\} \quad (35)$$

and

$$[\tilde{A}]\{\tilde{v}\} = \tilde{\lambda}\{\tilde{v}\} \quad (36)$$

Using the definition of $[\tilde{A}]$, Eq. (36) can be recast as

$$[A][R]\{\tilde{v}\} = \alpha\tilde{\lambda}[R]\{\tilde{v}\} \quad (37)$$

Comparing Eqs. (35) and (37), the following results are observed

$$\tilde{\lambda} = \frac{1}{\alpha}\lambda \quad (38)$$

and

$$\{\tilde{v}\} = [R]^{-1}\{v\} \quad (39)$$

Hence, it is clear that the eigenvalues of $[\tilde{A}]$ are simply the eigenvalues of $[A]$ scaled by factor $1/\alpha$. Therefore, if the original system is stable, the time scaled system will be stable also, because only positive real time scalings are allowed ($\alpha > 0$). Likewise, if the original system is unstable, the time scaled system also will be unstable. Nevertheless, the margins of stability are affected, as the eigenvalues grow or shrink depending on α .

V. Controllability and Observability Gramians

The unscaled system of equations has a controllability Gramian, $[W_c]$, which satisfies the following Lyapunov equation:

$$[A][W_c] + [W_c][A]^T + [B][B]^T = [0] \quad (40)$$

and an observability Gramian, $[W_o]$, which satisfies the following Lyapunov equation:

$$[A]^T[W_o] + [W_o][A] + [C]^T[C] = [0] \quad (41)$$

Likewise, the time scaled system of equations have Gramians which identically satisfy

$$[\tilde{A}][\tilde{W}_c] + [\tilde{W}_c][\tilde{A}]^T + [\tilde{B}][\tilde{B}]^T = [0] \quad (42)$$

and

$$[\tilde{A}]^T [\tilde{W}_o] + [\tilde{W}_o] [\tilde{A}] + [\tilde{C}]^T [\tilde{C}] = [0] \quad (43)$$

Substituting expressions for $[\tilde{A}]$ and $[\tilde{B}]$ into Eq. (42) gives

$$\frac{1}{\alpha} [R]^{-1} [A] [R] [\tilde{W}_c] + \frac{1}{\alpha} [\tilde{W}_c] [R] [A]^T [R]^{-1} + \frac{1}{\alpha^2} [R]^{-1} [B] [B]^T [R]^{-1} = [0] \quad (44)$$

The final result of this equation is obtained by multiplying through by α^2 and the pre- and post-multiplying each term by $[R]$ to give

$$\alpha [A] [R] [\tilde{W}_c] [R] + \alpha [R] [\tilde{W}_c] [R] [A]^T + [B] [B]^T = [0] \quad (45)$$

Comparing Eq. (45) to Eq. (40) allows $[\tilde{W}_c]$ to be identified as

$$[\tilde{W}_c] = \frac{1}{\alpha} [R]^{-1} [W_c] [R]^{-1} \quad (46)$$

The corresponding equation for the time scaled observability matrix is determined similarly and is given by

$$[\tilde{W}_o] = \frac{\alpha}{\beta^2} [R] [W_o] [R] \quad (47)$$

where β is given by Eq. (30).

VI. Balanced Realization

The goal in the present research is not only to perform time scaling for well-conditioned computation of the Gramians, but also to balance and transform the original system of equations in order to prevent errors from being introduced due to inconvenient and inconsistent units being used for the time scale. That is, the reduced state-space model is meant to be created in a form suitable for easy use later. For instance, it may be necessary to use $\alpha = 1000$ for the computation of the Gramians which means the time scale is in units of milliseconds if the original time unit is seconds. However, for archival purposes, it is much better to store the reduced order model with time units of seconds. That this can be easily achieved is demonstrated as follows.

The eigenvalue problem used to compute the transformation matrix for conventional balanced realization is determined for the unscaled state-space system as

$$[W_c] [W_o] [T] = [T] [\sigma^2] \quad (48)$$

where $[\sigma]$ is a diagonal matrix of eigenvalues. The corresponding equation for the transformed system is given by

$$[\tilde{W}_c] [\tilde{W}_o] [\tilde{T}] = [\tilde{T}] [\tilde{\sigma}^2] \quad (49)$$

That these two equations define equivalent eigenvalue problems is observed by substituting Eqs. (46) and (47) into Eq. (49) and simplifying to give

$$[W_c] [W_o] [R] [\tilde{T}] = [R] [\tilde{T}] [\beta^2 \tilde{\sigma}^2] \quad (50)$$

Hence,

$$[\tilde{\sigma}^2] = \left[\frac{1}{\beta^2} \sigma^2 \right] \quad (51)$$

and

$$[R] [\tilde{T}] = [T] \quad (52)$$

or

$$[\tilde{T}] = [R]^{-1} [T] \quad (53)$$

Equations (42) and (43) which are better conditioned than Eqs. (40) and (41) are solved for the time scaled Gramians. Then the eigenvalue problem given by Eq. (49) is solved. Finally, the original (unscaled) set of state-space equations are transformed and truncated using $[T]$ determined from Eq. (52). That is, once $[T]$ has been calculated, the generalized balanced realization of the state-space matrices are determined as

$$[\bar{A}] = [T]^{-1} [A] [T] \quad (54)$$

$$[\bar{B}] = [T]^{-1} [B] \quad (55)$$

$$[\bar{C}] = [C] [T] \quad (56)$$

$$[\bar{D}] = [D] \quad (57)$$

Note that resulting system involving $[\bar{A}]$, $[\bar{B}]$, $[\bar{C}]$, and $[\bar{D}]$ employs the original time scale units. Hence, the effects of time scaling do not affect the final state-space representation that is achieved. Rather, time scaling allows the balancing transformation to be computed using a better conditioned, albeit temporary state-space representation.

VII. Sensitivity of the Controllability Lyapunov Equation

In order to compare the sensitivity of the scaled system to the unscaled system, the sensitivity measure of Ref. 11 is applied to the controllability Lyapunov equations given by Eqs. (40) and (42). Let Eq. (42) be rewritten as

$$[\tilde{A}] [\tilde{W}_c] + [\tilde{W}_c] [\tilde{A}]^T + [\tilde{Q}] = [0] \quad (58)$$

where

$$[\tilde{Q}] = [\tilde{B}] [\tilde{B}]^T \quad (59)$$

Stable real systems with $[\Delta \tilde{A}]$, $[\Delta \tilde{W}_c]$, $[\Delta \tilde{Q}]$ are considered with

$$([\tilde{A}] + [\Delta \tilde{A}]) ([\tilde{W}_c] + [\Delta \tilde{W}_c]) + ([\tilde{W}_c] + [\Delta \tilde{W}_c]) ([\tilde{A}] + [\Delta \tilde{A}])^T + ([\tilde{Q}] + [\Delta \tilde{Q}]) = [0] \quad (60)$$

Let $[\tilde{H}]$ be the solution to Eq. (58) for the case when $[\tilde{Q}] = [I]$. That is,

$$[\tilde{A}] [\tilde{H}] + [\tilde{H}] [\tilde{A}]^T + [I] = [0] \quad (61)$$

The sensitivity measure is then¹¹

$$\frac{\|[\Delta \tilde{W}_c]\|_2}{\|[\tilde{W}_c] + [\Delta \tilde{W}_c]\|_2} \leq 2 \|[\tilde{A}] + [\Delta \tilde{A}]\|_2 \|[\tilde{H}]\|_2 \left[\frac{\|[\Delta \tilde{A}]\|_2}{\|[\tilde{A}] + [\Delta \tilde{A}]\|_2} + \frac{\|[\Delta \tilde{Q}]\|_2}{\|[\tilde{Q}] + [\Delta \tilde{Q}]\|_2} \right] \quad (62)$$

where $\|\cdot\|_2$ represents the spectral or 2-norm which is defined as

$$\|[S]\|_2 = \max \frac{\|[S]\{x\}\|_2}{\|\{x\}\|_2} \quad (63)$$

with

$$\|\{x\}\|_2 = \sqrt{\{x\}^T \{x\}} \neq 0 \quad (64)$$

In Eq. (62), it is assumed that $\|[\tilde{A}] + [\Delta \tilde{A}]\|_2$, $\|[\tilde{W}_c] + [\Delta \tilde{W}_c]\|_2$, and $\|[\tilde{Q}] + [\Delta \tilde{Q}]\|_2$ are all nonzero. Equation (62) is written in compacted notation as

$$LHS \leq RHS \quad (65)$$

VIII. Time Scaled Gramian Calculation

The Gramians are computed directly using the methodology presented in Ref. 12. Essentially in this method, the Schur decompositions of $[\tilde{A}]$ and $[\tilde{A}]^T$ are employed to transform the controllability and observability Lyapunov equations into a more manageable form as follows. The Schur decompositions for these two real matrices are given by

$$[\tilde{A}] = [\hat{U}_1] [\hat{V}_1] [\hat{U}_1]^T \quad (66)$$

$$[\tilde{A}]^T = [\hat{U}_2] [\hat{V}_2] [\hat{U}_2]^T \quad (67)$$

where $[\hat{U}_1]$ and $[\hat{U}_2]$ are both orthonormal matrices and $[\hat{V}_1]$ and $[\hat{V}_2]$ are real upper quasi-triangular matrices with diagonal block size of 1 or 2. Using these decompositions, the time scaled controllability Lyapunov equation can be rewritten as follows:

$$[\hat{V}_1] [\hat{W}_c] + [\hat{W}_c] [\hat{V}_2] + [\hat{Q}] = [0] \quad (68)$$

where

$$[\hat{Q}] = [\hat{U}_1]^T [\tilde{Q}] [\hat{U}_2] \quad (69)$$

and

$$[\hat{W}_c] = [\hat{U}_1]^T [\tilde{W}_c] [\hat{U}_2] \quad (70)$$

The solution is obtained by comparing the columns appearing in the individual terms of Eq. (68) to solve for $[\hat{W}_c]$. Then $[\tilde{W}_c]$ is calculated by re-arranging Eq. (70) as follows:

$$[\tilde{W}_c] = [\hat{U}_1] [\hat{W}_c] [\hat{U}_2]^T \quad (71)$$

The time scaled observability Gramian is calculated in a similar fashion. The reader is directed to Ref. 12 for a complete discussion of the algorithm details.

IX. Simple Wing Example Problem

The first example problem selected for this development is a simple wing with a control surface at the trailing edge. This configuration is shown in Fig. 1. A single measurement point at the wing tip is chosen to go along with the single input of the control surface deflection. The control surface mode and the first three elastic modes are shown in Fig. 2. The flight conditions consist of a Mach number of 0.3 and a dynamic pressure of 200 psi.

A. Three state solution

For the purposes of demonstrating the effect of scaling on the system matrices, a single elastic mode along with a single aerodynamic lag state is used. This gives a total of three states that must be evaluated. The unscaled system has the following $[A]$ and $[B]$ matrices:

$$[A] = \begin{bmatrix} 0 & 1 & 0 \\ -5.9409 \times 10^7 / \text{s}^2 & -13,233.2 / \text{s} & -1.1526 \times 10^6 / \text{s}^2 \\ 0 & 1 & -6821.76 / \text{s} \end{bmatrix} \quad (72)$$

and

$$[B] = \begin{bmatrix} 0 \\ -1.4939 \times 10^9 / \text{s}^2 \\ 0 \end{bmatrix} \quad (73)$$

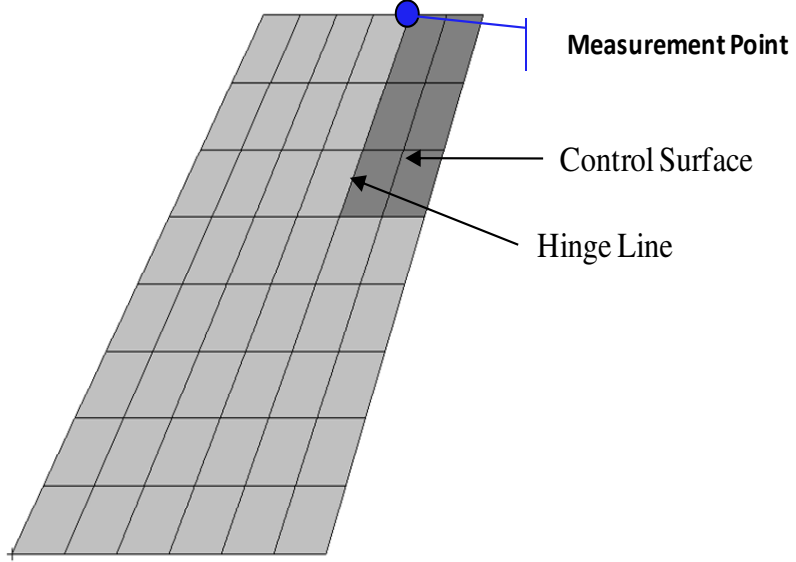


Figure 1. Simple wing geometry. The single measurement point at the wing tip is labeled.

Using $\alpha = 1000$ gives a scaled system where time is measured in milliseconds. The scaled $[A]$ and $[B]$ matrices for the time scaled system are

$$[\tilde{A}] = \begin{bmatrix} 0 & 1 & 0 \\ -59.409/\text{ms}^2 & -13.2332/\text{ms} & -1.1526/\text{ms}^2 \\ 0 & 1 & -6.82176/\text{ms} \end{bmatrix} \quad (74)$$

and

$$[\tilde{B}] = \begin{bmatrix} 0 \\ -1493.9/\text{ms}^2 \\ 0 \end{bmatrix} \quad (75)$$

Considering displacement to be the output of interest, the following matrices complete the unscaled and scaled systems:

$$[C] = [\tilde{C}] = [\Phi \ 0 \ 0] \quad (76)$$

and

$$[D] = [\tilde{D}] = [0] \quad (77)$$

It is clear from inspection that the time scaled system is much better conditioned than the unscaled system. Table 1 shows the values for the left and right hand sides of Eq. (62) for the controllability problem considering all non-identity entries in $[A]$ and $[B]$ to be altered by 1%. More specifically, $[A]$ and $[B]$ are modified and the corresponding modifications to $[\tilde{A}]$ and $[\tilde{B}]$ are found using their definitions. That is,

$$[\Delta \tilde{A}] = \frac{1}{\alpha} [R]^{-1} [\Delta A] [R] \quad (78)$$

and

$$[\Delta \tilde{B}] = \frac{1}{\alpha} [R]^{-1} [\Delta B] \quad (79)$$

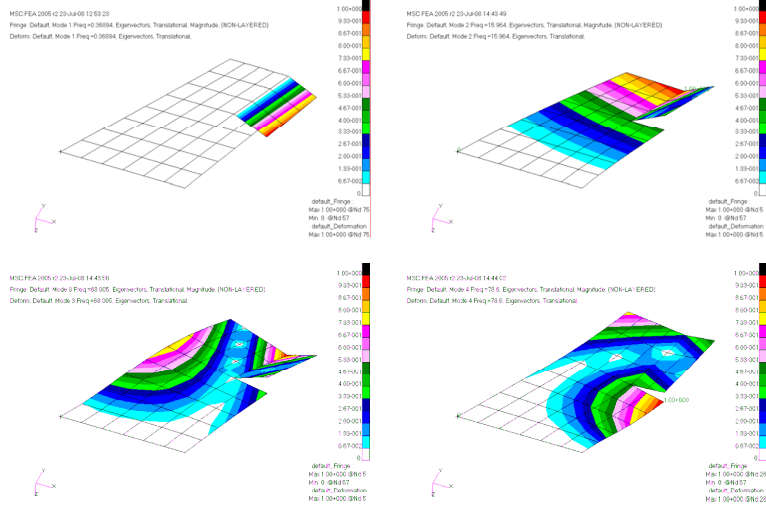


Figure 2. Control surface mode and first three elastic modes.

Note that the left hand side of Eq. (62) which is the relative change in controllability Gramian is not exactly 0.01, because the identity entry in $[A]$ is left unmodified. The condition number of $[\tilde{A}]$ is also shown in Table 1, along with normalized error measures for the controllability and observability Lyapunov equations which are defined as

$$\epsilon_c \equiv \frac{\left\| [\tilde{A}] [\tilde{W}_c] + [\tilde{W}_c] [\tilde{A}]^T + [\tilde{B}] [\tilde{B}]^T \right\|_F}{\left\| [\tilde{A}] \right\|_F} \quad (80)$$

and

$$\epsilon_o \equiv \frac{\left\| [\tilde{A}]^T [\tilde{W}_o] + [\tilde{W}_o] [\tilde{A}] + [\tilde{C}]^T [\tilde{C}] \right\|_F}{\left\| [\tilde{A}] \right\|_F} \quad (81)$$

where $\|\cdot\|_F$ represents the Frobenius norm which is defined as follows for real matrices:

$$\|[S]\|_F = \sqrt{\sum_{i=1}^m \sum_{j=1}^n |S_{ij}|^2} = \sqrt{\text{trace}([S]^T [S])} \quad (82)$$

Table 1. Conditioning of the three state system.

α	<i>LHS</i>	<i>RHS</i>	$\text{cond}([\tilde{A}])$	ϵ_c	ϵ_o
1.0	0.0099	7.907×10^9	5.9420×10^7	1.4551×10^6	7.4752×10^{-23}
1000.0	0.0099	8.7303	63.0554	2.4872×10^{-11}	3.0492×10^{-17}

Although using the unscaled system ($\alpha = 1$) along with the algorithm from Ref. 12 produces correct results for the observability Gramian ($\epsilon_o \approx 0$), the results for the controllability Gramian are quite in error

$(\epsilon_c \gg 0)$. Using a scaling of $\alpha = 1000$ produces results that are much better behaved. It is also noted that the bound on the relative change in the Gramian (*RHS*) decreases dramatically in going from $\alpha = 1$ to $\alpha = 1000$.

B. Forty state solution

Here a total of eight elastic modes and three aerodynamic lag states per elastic mode are used. The magnitude of the frequency response of the wing tip deflection as a function of the control surface excitation is shown in Fig. 3. Also shown in Fig. 3 is the magnitude of the frequency response for the balanced truncated system where 17 of the 40 possible states are used. As is evident from examining the figure, excellent results have been obtained from the balanced and truncated system.

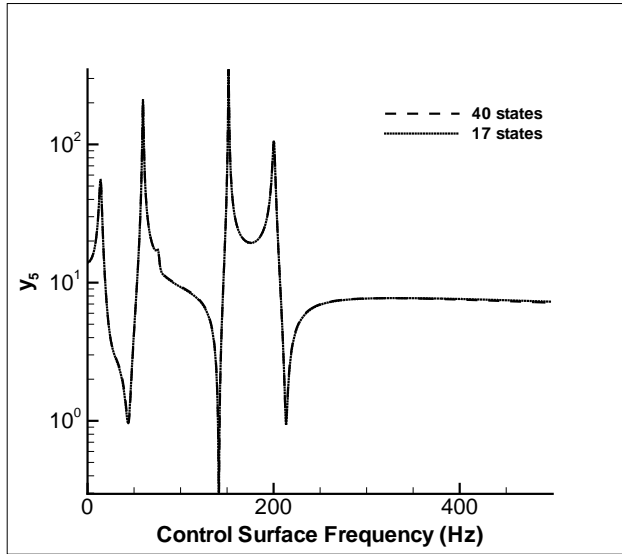


Figure 3. Magnitude of the frequency response of the wing tip deflection as a function of the control surface frequency for the full and truncated systems.

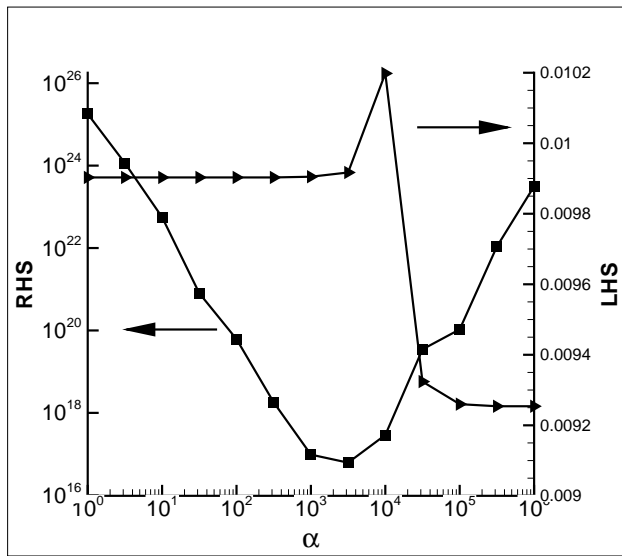


Figure 4. Sensitivity of the 40 state system.

Results for the left and right hand sides of Eq. (62) are shown in Fig. 4. It is noted that the bound provided by Eq. (62) is not very tight for this larger system, even when significant scaling is applied. Nevertheless, the bound appears to be best for a value of α near 10^3 .

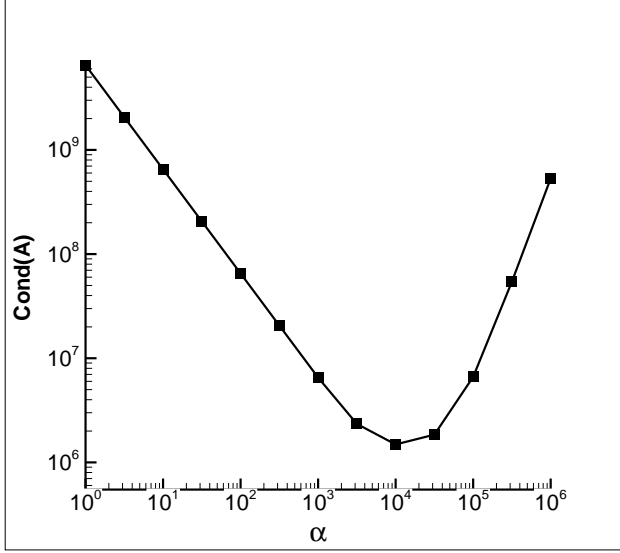


Figure 5. Condition of $[\tilde{A}]$ for the 40 state system.

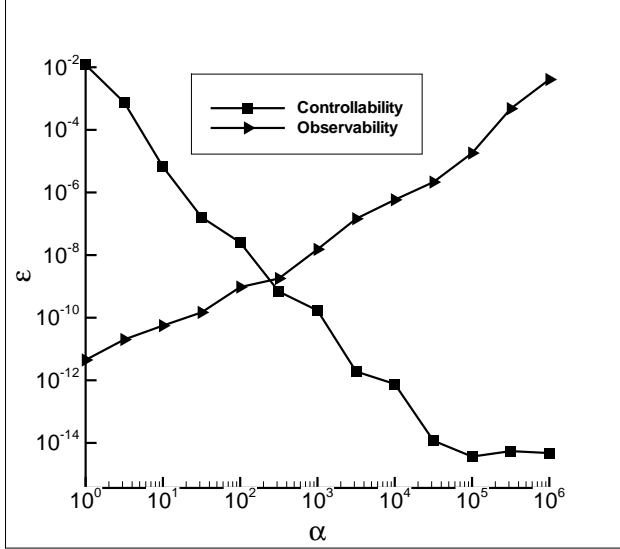


Figure 6. Relative error in solving the Lyapunov equations for the 40 state system.

The condition number of $[\tilde{A}]$ is shown in Fig. 5 and the relative errors in solving the Lyapunov equations for the Gramians are shown in Fig. 6. The condition of $[\tilde{A}]$ appears to be optimal near $\alpha = 10^4$. The error in the controllability and observability Gramians show opposite trends with α . An optimal value considering the controllability and observability Gramians equally appears to be near $\alpha = 200$. The final choice of α depends on the problem at hand. Nevertheless, there are large ranges in α that are acceptable.

X. S4T Example Problem

The S4T configuration is a scaled version of a supersonic transport configuration developed by NASA, Boeing, and McDonnell Douglas known as the Technology Concept Aircraft (TCA). A photograph of the S4T model is shown in Fig. 7. This model is 16 ft long representing a 4.91% scaled version of the TCA. The mass and stiffness of the model have been tailored to achieve dynamically scaled structural behavior.¹³ The model is constructed with a graphite-epoxy flexible fuselage beam, fiberglass-epoxy/honeycomb sandwich wing, and graphite-epoxy control surfaces. In order to represent the structural dynamics of the TCA fuselage, the flexible fuselage beam is mounted to a stiff aluminum channel through springs at four locations. This aluminum channel is referred to as the rigid beam and is connected through a balance to the wind tunnel wall. The model has three actuated control surfaces, variable mass engine nacelles, and instrumentation to measure acceleration, strain, and pressure.



Figure 7. S4T model.

The S4T model is instrumented with 43 accelerometers, 6 strain gages, and 55 pressure taps. Based on the results of some open loop testing, eight sensors are selected which had relatively high coherence and transfer magnitude at frequencies corresponding to the two lowest frequency modes. The accelerometers chosen for this study are shown in Fig. 8.

Actuation of the S4T model is addressed with three aerodynamic control surfaces. This includes an aileron/flap, horizontal tail, and a canard or ride control vane. The location of these control surfaces are shown in Fig. 9.

The flight conditions are given by a Mach number of 0.8, a dynamic pressure of 0.277778 psi, and a flight velocity of 5079.0 in/s. The aerodynamics are represented using the doublet-lattice method. A total of 30 structural modes and 2 aerodynamic lags are used to represent the S4T model. This results in a total of 120 states to go along with the 8 chosen outputs and 3 inputs. A total of 24 transfer functions exist with a representative set shown in Fig. 10 for the acceleration of the aft wing tip point as a function of the canard, aileron/flap, and horizontal tail inputs. Using the full 120 states or truncating to 20 states produces the same results.

The condition number of \tilde{A} is shown in Fig. 11. Based on the condition number alone, the optimal time scaling appears to be $\alpha = 10^4$. The relative error in calculating the Gramians from the Lyapunov

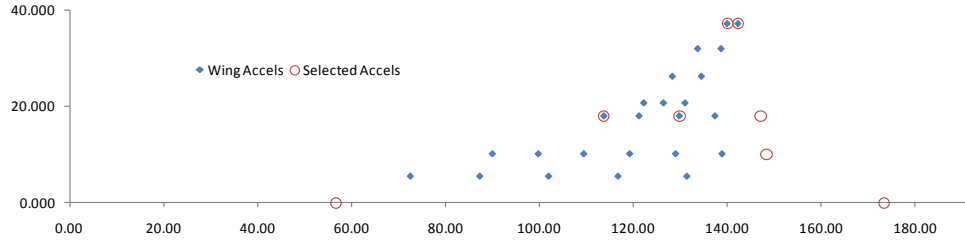


Figure 8. Location of selected accelerometers (inches).

equations (Eqs. (80) and (81)) are shown in Fig. 12. The relative error in calculating $[\widetilde{W}_c]$ shows an overall downward trend with increasing α . Here, three separate error measures for the observability Gramian are computed based on whether the displacement, velocity, or acceleration is chosen as the output. Similar to the simple wing example, when displacement is chosen as the output, the controllability and observability errors have opposite trends with increasing α . The relative error in computing $[\widetilde{W}_o]$ for acceleration output has a similar trend to that for $[\widetilde{W}_c]$. Finally, the trend for ϵ_o for velocity output falls in between that for displacement and acceleration output. Considering displacement or velocity output, the optimal value (i.e., the value that weights ϵ_c and ϵ_o equally) appears to be $\alpha = 10^2$, whereas for acceleration output, an α of 10^5 minimizes ϵ_o .

Once again, even though the optimal value of α is not coincident when considering the condition number of $[\widetilde{A}]$, ϵ_c , and ϵ_o , there appears to be a wide range of values that produce acceptable errors in calculating $[\widetilde{W}_c]$ and $[\widetilde{W}_o]$.

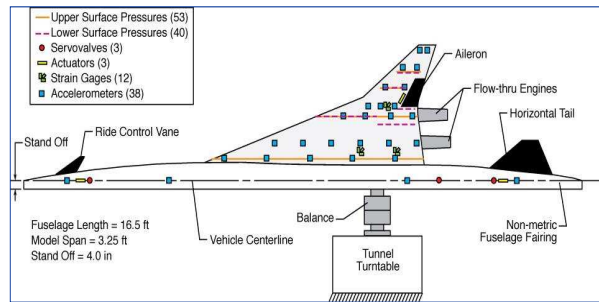


Figure 9. Location of control surfaces.

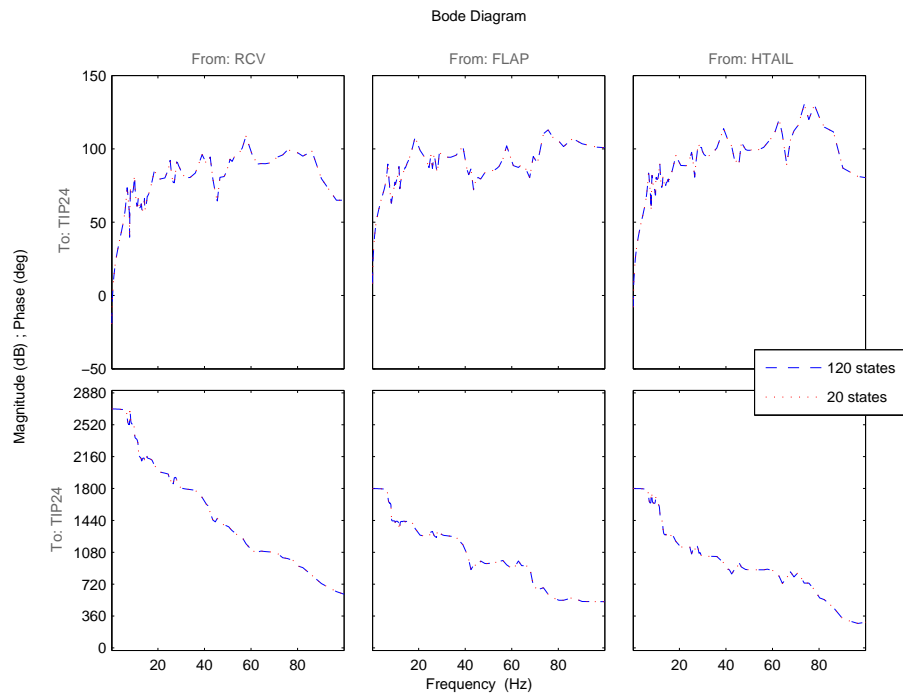


Figure 10. Bode plots of from the three inputs to the aft wing tip deflection.

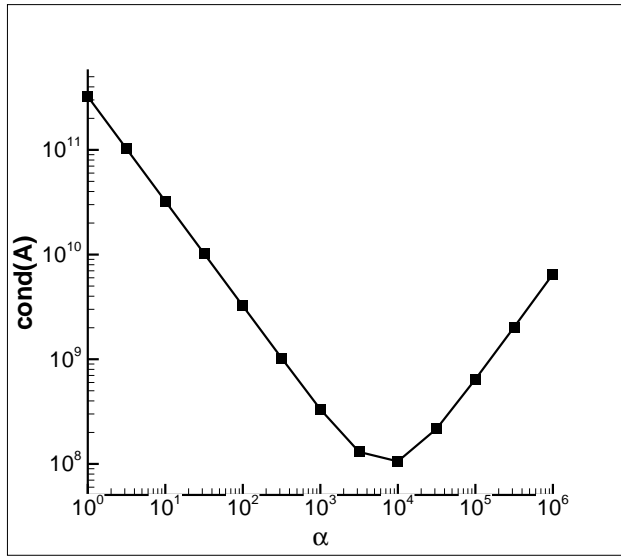


Figure 11. Condition number of \tilde{A} as a function of scaling parameter α for the 120 state solution.

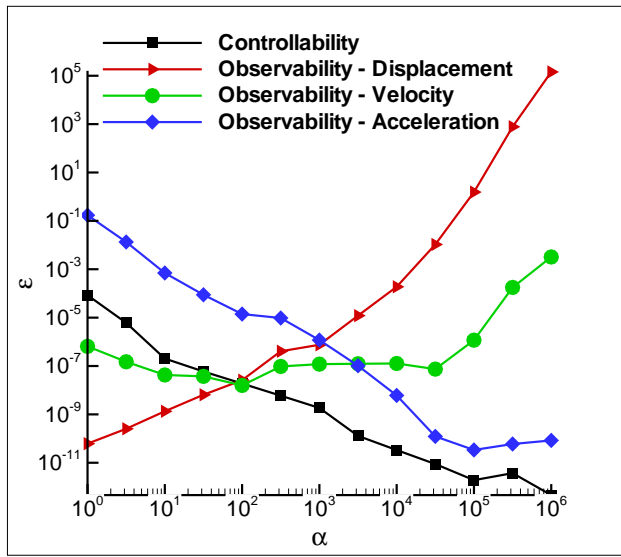


Figure 12. Relative error in solving the Lyapunov equations for the Gramians of the 120 state system. Errors for the case where displacement, velocity, or acceleration are taken as the output are shown.

XI. Conclusions

A methodology for time scaling aeroservoelastic state-space equations has been presented. This time scaling leads to better conditioned Lyapunov equations which can be solved for controllability and observability Gramians which subsequently can be used to create a balanced and truncated reduced order model appropriate for archival purposes. The optimal value of time scaling is problem and output dependent, but large ranges of acceptable values likely exist.

XII. Acknowledgment

Funding for this development has been provided by the Aeroelasticity Branch of NASA Langley Research Center. The NASA technical representative for this research is Walter A. Silva.

References

¹Baker, M. and Lenkey, P., "Parametric Flutter Analysis of the TCA Configuration and Recommendation for FFM Design and Scaling," McDonnell Douglas Report CRAD-9306-TR-3088.

²Fogarty, T. and Baker, M., "MSC/NASTRAN Flutter Analysis of TCA with Lateral and Directional Control Laws," HSR Program Memorandum, 1998.

³Perry, B., Silva, W., Florance, J., Wieseman, C., Pototzky, A., Sanetrik, M., Scott, R., Keller, D., and Cole, S., "Plans and Status of Wind-Tunnel Testing Employing an Aeroservoelastic Semispan Model," *48th AIAA/ASME/ASCE/AHS/ASC Structures, Structural Dynamics, and Materials Conference*, Honolulu, HI, 2007.

⁴Roughen, K. M., Bendiksen, O. O., and Baker, M. L., "Development of Generalized Aeroservoelastic Reduced Order Models," *50th AIAA/ASME/ASCE/AHS/ASC Structures, Structural Dynamics, and Materials Conference*, Palm Springs, CA, 2009.

⁵Moore, B. C., "Principal Component Analysis in Linear Systems: Controllability, Observability, and Model Reduction," *IEEE Transactions on Automatic Control*, Vol. 26, 1981, pp. 17–32.

⁶Laub, A., Heath, M., Paige, C., and Ward, R., "Computation of System Balancing Transformations and Other Applications of Simultaneous Diagonalization Algorithms," *IEEE Transactions on Automatic Control*, Vol. 32, No. 2, 1987, pp. 115–122.

⁷Tombs, M. and Postlethwaite, I., "Truncated Balanced Realization of a Stable Non-Minimal State-Space System," *International Journal of Control*, Vol. 46, No. 4, 1987, pp. 1319–1330.

⁸Giesing, J., Kalman, T., and Rodden, W., "Subsonic Unsteady Aerodynamics for General Configuration," AFFDL-TR-71-5, 1971.

⁹Rodden, W., Harder, R., and Bellinger, E., "Aeroelastic Addition to NASTRAN," NASA CR-3094, 1979.

¹⁰Roger, K., "Airplane Math Modeling Methods for Active Control Design," AGARD-CP-228 Structural Aspects of Active Controls, 1977.

¹¹Hewer, G. and Kenney, C., "The Sensitivity of the Stable Lyapunov Equation," *SIAM Journal on Control and Optimization*, Vol. 26, No. 2, 1988, pp. 321–344.

¹²Sorensen, D. and Zhou, Y., "Direct Methods for Matrix Sylvester and Lyapunov Equations," *Journal of Applied Mathematics*, Vol. 2003, No. 6, 2003, pp. 277–303.

¹³Baker, M. and Lenkey, P., "Parametric Flutter Analysis of the TCA Configuration and Recommendation for FFM Design and Scaling," McDonnell Douglas Report CRAD-9306-TR-3088.